


Article

A Highly Selective and Sensitive Fluorescent Turn-Off Probe for Cu²⁺ Based on a Guanidine Derivative

Fei Ye, Qiong Chai, Xiao-Min Liang, Ming-Qiang Li, Zhi-Qiang Wang and Ying Fu * 

Department of Applied Chemistry, College of Science, Northeast Agricultural University, Harbin 150030, China; yefei@neau.edu.cn (F.Y.); chaiqiong01@163.com (Q.C.); abcliangxiaomin@163.com (X.-M.L.); mqli@neau.edu.cn (M.-Q.L.); wzq19910101@163.com (Z.-Q.W.)

* Correspondence: fuying@neau.edu.cn; Tel.: +86-451-5519-0070

Received: 16 September 2017; Accepted: 13 October 2017; Published: 16 October 2017

Abstract: A new highly selective and sensitive fluorescent probe for Cu²⁺, *N*-*n*-butyl-4-(1'-cyclooctene-1',3',6'-triazole)-1,8-naphthalimide (**L**), was synthesized and evaluated. The structure of compound **L** was characterized via IR, ¹H-NMR, ¹³C-NMR and HRMS. The fluorescent probe was quenched by Cu²⁺ with a 1:1 binding ratio and behaved as a “turn-off” sensor. An efficient and sensitive spectrofluorometric method was developed for detecting and estimating trace levels of Cu²⁺ in EtOH/H₂O. The ligand exhibited excitation and emission maxima at 447 and 518 nm, respectively. The equilibrium binding constant of the ligand with Cu²⁺ was 1.57 × 10⁴ M⁻¹, as calculated using the Stern-Volmer equation. Ligand **L** is stable and can be used to detect Cu²⁺ in the range of pH from 7 to 12. The sensor responded to Cu²⁺ rapidly and a large number of coexisting ions showed almost no obvious interference with the detection.

Keywords: fluorescence; naphthalimide; guanidine; octatomic ring; copper ion

1. Introduction

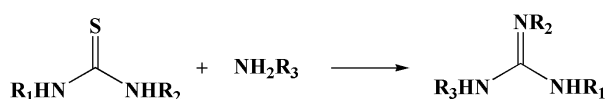
Fluorescent sensors for chemical species used in biological and environmental detection are currently an attractive field of research [1–3]. In particular, pollution by heavy metal ions has attracted much attention because these metal ions not only play important roles in various physiological processes but also have distinctly toxic impact on human health [4]. It is highly desired to detect these in relevant systems. The importance of metal ion sensing can never be overestimated because of their widespread distribution in environmental systems and biological processes [5]. Copper is a significant metal pollutant because of its widespread application and is also an essential trace element in biological systems. Cu²⁺ is present in various biological processes, as the third most abundant transition metal ion in the human body. In addition, its homeostasis is critical for the metabolism and development of living organisms [6–8]. For example, Cu²⁺ plays a critical role as a catalytic cofactor for a variety of metalloenzymes, including superoxide dismutase, cytochrome oxidase and tyrosinase [9,10]. The misregulation or excess accumulation of Cu²⁺ could cause serious diseases [11]. Its concentration in the neuronal cytoplasm may contribute to the etiology of Alzheimer's or Parkinson's disease [12–14]. However, exposure to high levels of Cu²⁺ will cause gastrointestinal disturbance and even liver or kidney damage. The detection of Cu²⁺ is meaningful for both disease diagnosis and environmental monitoring [15]. The normal average concentration of Cu²⁺ in blood is in the range of 15.7–23.6 μM [16]. The U.S. Environmental Protection Agency (EPA) set a limit for Cu²⁺ in drinking water of 20 μM [17]. The detection of Cu²⁺ levels in water requires an efficient, selective and highly sensitive chemosensor [18,19].

Numerous methods to detect metal ions have been developed, such as atomic absorption spectrometry [20], inductively coupled plasma atomic emission spectroscopy [21], visual detection [22,23], chemiluminescence detection [24] and electrochemical techniques [25,26]. However, these methods have disadvantages, such as expensive instrumentation, complicated sample preparation and tedious operating procedures, resulting in the need for other sensitive, simple detection methods for copper ions. Fluorescent molecules offer many advantages over other systems in this area as a result of their emissive behavior, easy signal detection, sensitivity, selectivity and low cost [27,28]. The development of the fluorescence method has been demonstrated to be promising because of its advantages of wide applicability, ease of manipulation, high selectivity, sensitivity, rapidity, nondestructive methodology and direct visual perception [29,30]. Thus, a number of high-performance sensors have been developed to detect metal ions [31]. Cu^{2+} is a typical ion with a pronounced quenching effect on fluorophores via mechanisms that are inherent to the paramagnetic species [32–35].

Many excellent chemosensors have been reported for Cu^{2+} in the past few years. However, many of these sensors only exhibit sensitive and selective Cu^{2+} detection in pure organic systems (Table 1) [36–38]. Hence, we designed and synthesized a new fluorescent sensor, *N-n*-butyl-4-(1'-cyclooctene-1',3',6'-triazole)-1,8-naphthalimide, based on the transformation of thiourea into guanidine derivatives, as shown in Scheme 1. This novel compound has a highly sensitive fluorescent response toward Cu^{2+} in mixed aqueous solutions.

Table 1. Comparison of the recently reported sensors for the determination of Cu^{2+} ions.

Operation Mode	Solvent	$\lambda_{\text{ex}}/\lambda_{\text{em}}$ (nm)	Interference	References
Turn-off	CH_3CN	364/420	None	[36]
Turn-on	CH_3CN	365/475	Zn(II)	[37]
Turn-off	MeOH	480/518	None	[38]
Turn-off	EtOH/ H_2O	437/518	None	This work



Scheme 1. Thiourea transformation into guanidine.

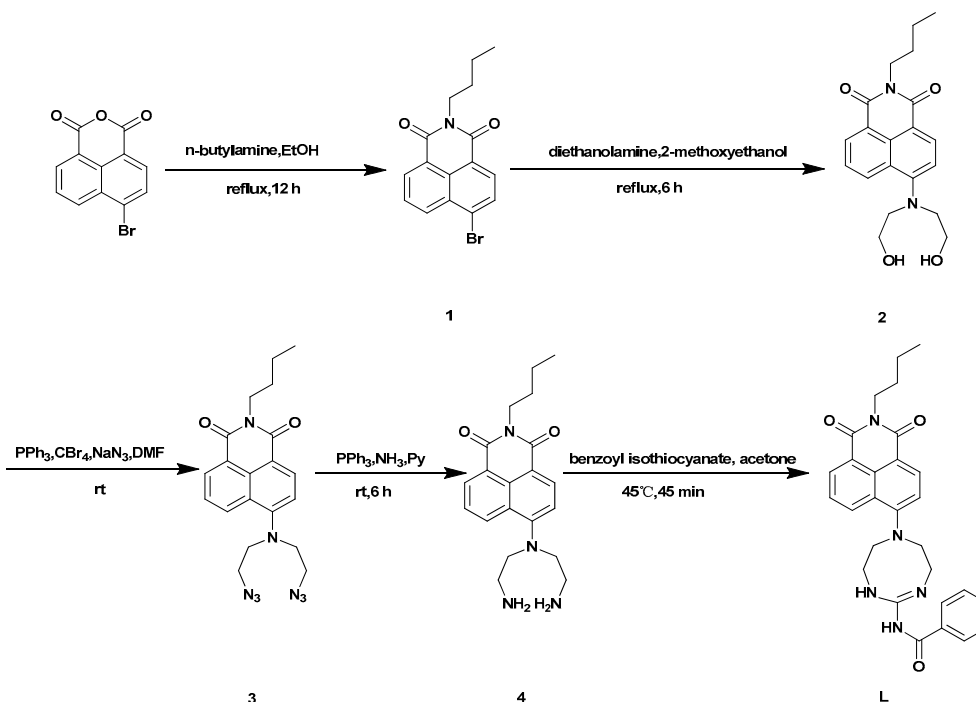
2. Results and Discussion

2.1. Synthesis and Characterization

Compound **L** was synthesized through the route outlined in Scheme 2. The structure modification was focused on the C-4 position. A dihydroxyethylamino moiety was introduced to replace the Br atom, and the subsequent reaction modified the -OH group to N_3 ; compound **4** was obtained in a 67% yield from the amination. Thiourea is easily transformed into guanidine; however, the conversion from thiourea to guanidine has attracted little attention as a potential fluorogenic reaction because most thiourea derivatives have the same color or fluorescence as their guanidine analogues [39]. Initially, we envisioned that a similar molecular recognition/reactivity motif might be incorporated into fluorophores to serve as a ratiometric fluorescent chemodosimeter for the selective detection of Hg^{2+} , as reported in the literature [40], because compound **4** has two free amino groups. The expected thiourea derivative was not achieved; however, the product transformed into the inner guanidine ring because compound **4** contained a primary amine subunit. Compound **L** was obtained through intramolecular cyclization with a recognition/reactivity motif that could be incorporated into fluorophores so that metal ion addition led to a variation of the fluorescence.

Compound **L** was obtained with a yield of 57% in the final reaction, and its structure was characterized by $^1\text{H-NMR}$, $^{13}\text{C-NMR}$ and HRMS. As evidenced by the signals at 6.57–8.42 ppm in

the $^1\text{H-NMR}$ spectrum, the number of Ar-H is 10, which indicated that benzoyl isothiocyanate had reacted with compound **4**. The signals at $\delta = 9.02$ ppm indicated the existence of benzamide, and the signals at $\delta = 1.26$ ppm showed that $-\text{NH}_2$ was substituted. Furthermore, the molecular ion peak in the HRMS-ESI ($[\text{M} + \text{H}]^+$, $484.2332 m/z$) spectrum was consistent with the theoretically calculated molecular mass of compound **L**.



Scheme 2. Synthetic route to compound **L**.

2.2. Spectral Characteristics

The photophysical characteristics of compound **L** in EtOH/ H_2O (4:1 v/v) were investigated. Figure 1 shows the excitation ($\lambda = 447$ nm) and emission ($\lambda = 518$ nm) spectra of compound **L**. The Stokes shift ($\nu_A - \nu_F$), an important parameter indicating the difference in properties and structure between the ground state (S_0) and first excited state (S_1), was calculated by Equation (1) to be 3062 cm^{-1} .

$$(\nu_A - \nu_F) = (1/\lambda_A - 1/\lambda_F) \times 10^{-7} \text{ cm}^{-1} \quad (1)$$

The ability of the molecules to emit absorbed light energy is characterized quantitatively by the fluorescence quantum yield (Φ_F). The quantum yields of fluorescence were calculated using coumarin 6G ($\Phi_{\text{sample}} = 0.94$) in EtOH as the standard according to Equation (2), where A_{ref} , S_{ref} , and n_{ref} and A_{sample} , S_{sample} , and n_{sample} represent the absorbance at the excited wavelength, the integrated emission band area and the solvent refractive index of the standard and the sample, respectively [41,42]. Thus, the fluorescence quantum yield of probe **L** in EtOH/ H_2O (4:1 v/v) solution was 0.06.

$$\Phi_F = \Phi_{\text{ref}} \left(\frac{S_{\text{sample}}}{S_{\text{ref}}} \right) \left(\frac{A_{\text{ref}}}{A_{\text{sample}}} \right) \left(\frac{n_{\text{sample}}^2}{n_{\text{ref}}^2} \right) \quad (2)$$

The photophysical properties of compound **L** as a ligand in the presence of different metal cations were investigated in EtOH/ H_2O (4:1 v/v) to determine its potential application as a sensor for detecting these metal ions. The binding behavior of compound **L** toward different metal ions such as their corresponding chlorides, acetates, sulfides or nitrates was studied using fluorescence spectroscopy. The anions did not affect the spectroscopic results.

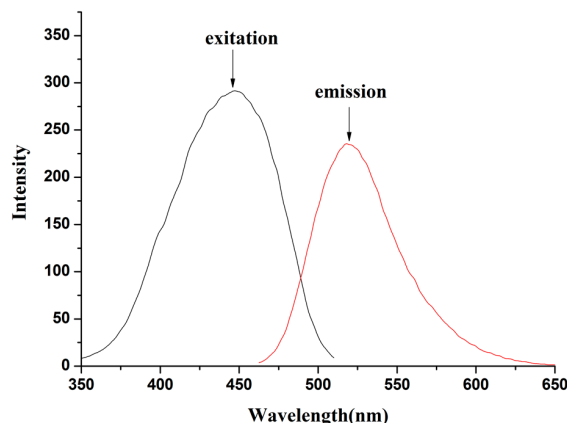


Figure 1. Excitation and emission spectra of compound L (10 μM) in EtOH/H₂O (4:1 *v/v*).

To evaluate the selectivity of compound L for Cu²⁺, changes in the fluorescence intensity upon the addition of various metal ions under the same conditions were investigated. The fluorescence spectrum of compound L exhibited strong fluorescence emission when excited at 447 nm in EtOH/H₂O (4:1 *v/v*; Figure 2). Under the same conditions as those used for adding the metal ions, significant fluorescence changes were observed in the presence of Cu²⁺. Fluorescence quenching was observed immediately after Cu²⁺ was added. When other metal ions were added, the fluorescence exhibit few changes. As shown in Figure 2, remarkable color changes ranging from yellow to colorless and yellow flocules floating in the solution could be distinguished by the naked eye. In addition, the introduction of Cu²⁺ to the mixture solution of compound L led to evident fluorescence quenching, while the rest of the metal cations exerted a negligible or very small influence under identical conditions, which was further evidenced by the illumination taken under a 365 nm portable UV lamp. On the basis of the literature, the fluorescence quench of probe L might have been due to the coordination to paramagnetic Cu²⁺ [43].

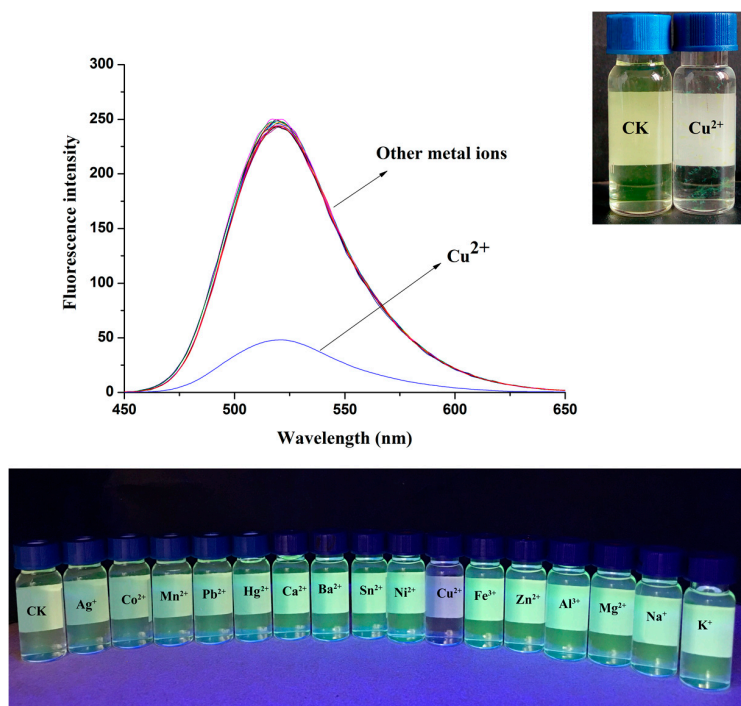


Figure 2. Fluorescence changes of compound L (10 μM) in the absence (CK) and presence of metal cations (50 μM) in EtOH/H₂O (4:1 *v/v*).

2.3. Calculation of Binding Constants and Different Concentrations of Cu^{2+}

A Job plot was generated by continuously varying the mole fraction of Cu^{2+} from 0 to 1 in a solution of $[\text{L-Cu}^{2+}]$ with a total concentration of $50 \mu\text{M}$ to determine the stoichiometry of the $[\text{L-Cu}^{2+}]$ complex. The Job plot analysis revealed an approximate maximum at a 0.5 mole fraction, which indicated a 1:1 stoichiometry of the ligand **L** and Cu^{2+} complex (Figure 3).

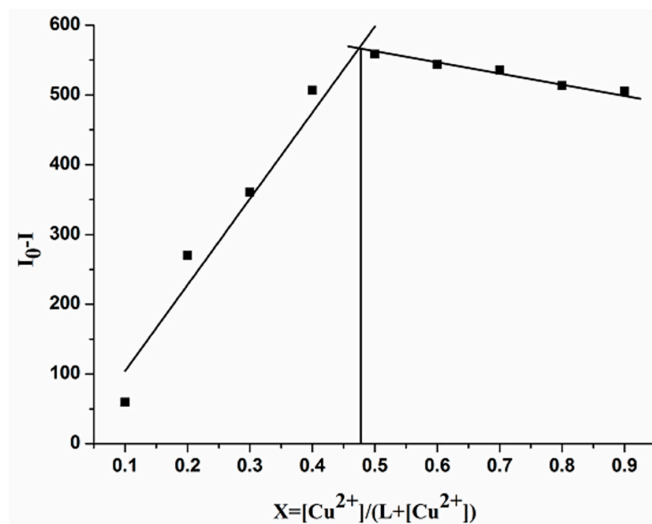


Figure 3. Job plot to determine the stoichiometry of the $[\text{L-Cu}^{2+}]$ complex in solution.

To better understand the sensing process, changes in the fluorescence spectra of compound **L** were measured along with the binding constant and different concentrations of Cu^{2+} . The binding constant was calculated using the Stern-Volmer equation, $I_0/(I_0 - I) = 1/A + 1/KA \cdot 1/[Q]$, on the basis of a 1:1 stoichiometry, where I_0 is the fluorescence intensity of the free ligand **L**, I is the fluorescence intensity of the L-Cu^{2+} complex, Q is $[\text{Cu}^{2+}]$, A is a constant and K is a binding constant [44]. When the reciprocal of $I_0/(I_0 - I)$ was plotted as a function of the $1/[Q]$ concentration, a linear relationship was obtained, ($y = A + Bx$), $y = I_0/(I_0 - I)$, $A = 1/A$, $B = 1/KA$, $x = 1/[Q]$, and K was calculated from A/B (Figure 4). Therefore, K , the binding association constant for Cu^{2+} , was estimated to be $1.57 \times 10^4 \text{ M}^{-1}$ in the EtOH/ H_2O (4:1 v/v) solution, as inferred from the fluorescence titration curves of compound **L** with Cu^{2+} .

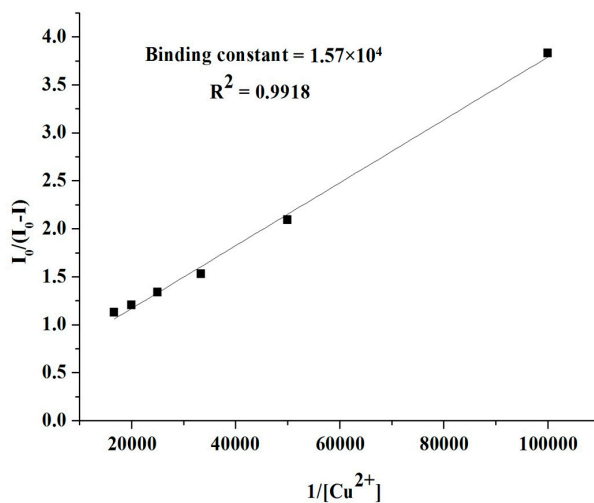


Figure 4. Stern-Volmer plot for calculating the binding constant of the chemosensor with Cu^{2+} .

Upon the addition of Cu^{2+} , the fluorescence was quenched. The changes in the fluorescence emission intensities of compound **L** ($1 \times 10^{-5} \text{ mol L}^{-1}$) with different concentrations of Cu^{2+} ($0\text{--}3 \times 10^{-4} \text{ mol L}^{-1}$) are presented in Figure 5. A progressive decrease in the fluorescence intensity was observed. The plot of the fluorescence intensity versus externally added Cu^{2+} (Figure 6) reaches saturation after a certain amount of externally added Cu^{2+} . Curvilinearity was obtained for up to a value of 6 times ($6 \times 10^{-5} \text{ mol L}^{-1}$) the amount of externally added Cu^{2+} . The results indicated that compound **L** could detect Cu^{2+} at a micromole level.

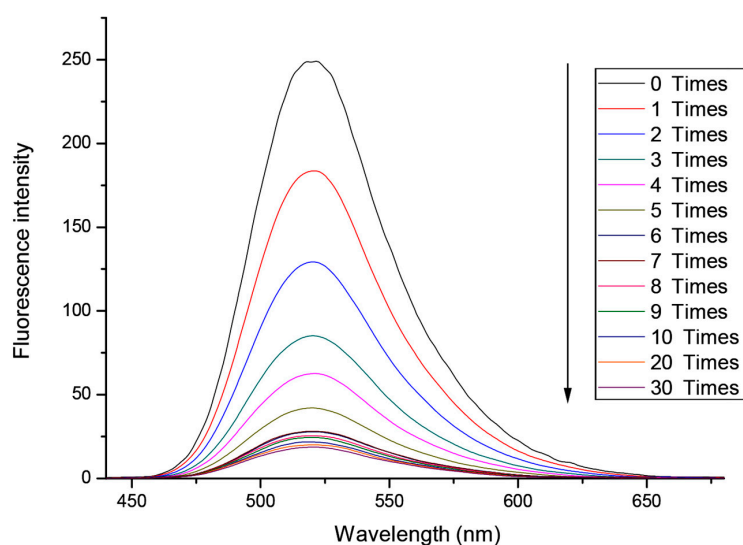


Figure 5. Changes in the fluorescence spectra of compound **L** ($10 \mu\text{M}$) in EtOH/ H_2O (4:1 *v/v*) as a function of added $[\text{Cu}^{2+}]$.

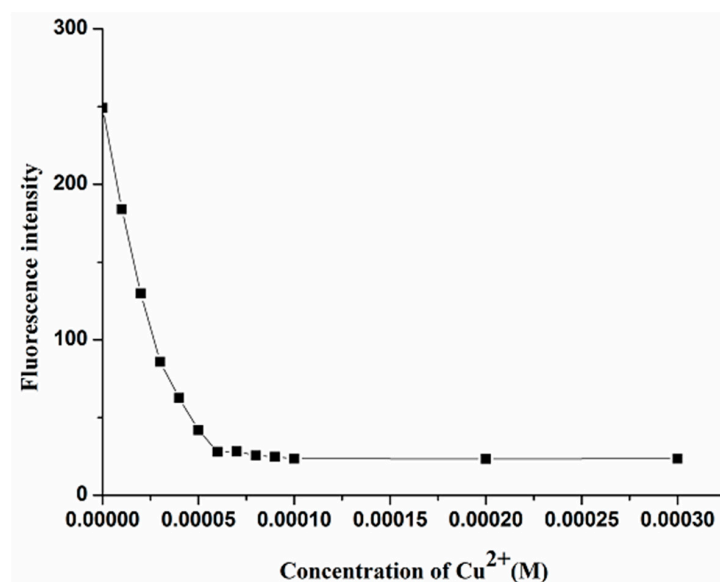


Figure 6. Fluorescence intensity vs Cu^{2+} ; inset shows that up to 6-fold Cu^{2+} curvilinearity was sustained; λ_{ex} : 437 nm; λ_{em} : 518 nm; slit width: 10 nm.

2.4. Response Time

The response time is a significant practical parameter [45]. Time-dependence of probe **L** for sensing Cu^{2+} was examined and the results are illustrated in Figure 7. Upon the addition of Cu^{2+} , the fluorescence intensity decreased to the minimum immediately and tended to be stable during the

test time. No changes in the fluorescence of probe L in the absence of Cu^{2+} were detected with the increased time. This showed that probe L exhibited a reliable rapid response to Cu^{2+} .

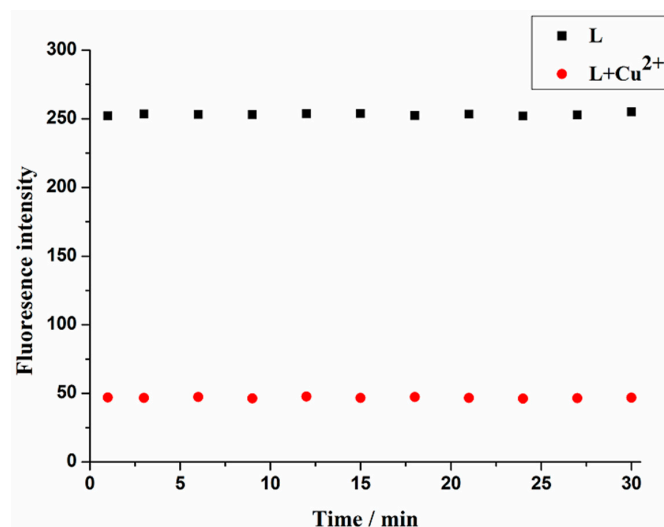


Figure 7. Response time of 10 μM probe L in the absence or presence of 50 μM Cu^{2+} in EtOH/ H_2O (4:1 v/v); λ_{ex} : 437 nm; λ_{em} : 518 nm; slit width: 10 nm.

2.5. Effect of pH

In order to investigate the application of probe L within complex media, the fluorescence spectra response of probe L was measured in the absence or presence of $5 \times 10^{-5} \text{ mol L}^{-1} \text{ Cu}^{2+}$ under different pH conditions. As shown in Figure 8, the fluorescence intensity of probe L did not reveal any clear differences over a pH range of 2–12, which was consistent with the goal of our experimental design. The fluorescence of the $[\text{L}-\text{Cu}^{2+}]$ solution could not remarkably decrease when the pH values were lower than 5, possibly because the imino groups of probe L were protonated at acid conditions, resulting in weak coordination with Cu^{2+} . In addition, the fluorescence intensity of the $[\text{L}-\text{Cu}^{2+}]$ solution showed a 5-fold change from pH 4 to pH 7, which suggested that it is sensitive to pH changes. These results indicated that probe L could be used to detect biological as well environmental Cu^{2+} in the range of pH from 7 to 12.

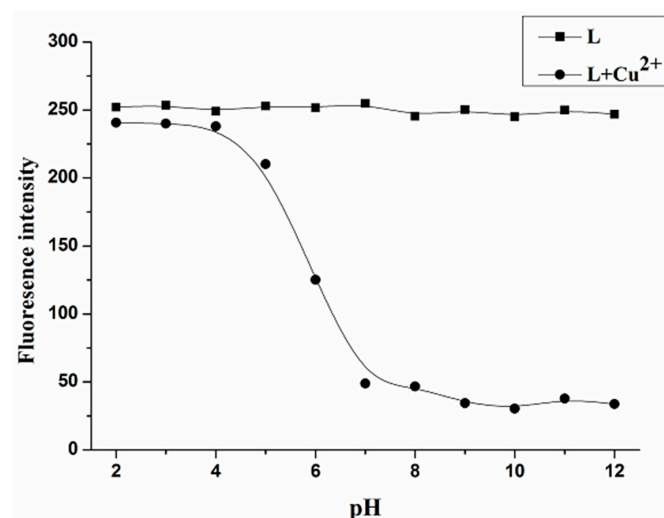


Figure 8. Effect of pH on the fluorescence intensity of 10 μM probe L in the absence or presence of 50 μM Cu^{2+} .

2.6. Selectivity

The selectivity is clearly one of the most important characteristics of a cation-selective chemosensor. Thus, the influence of other metal ions on the fluorescence intensity of the proposed Cu^{2+} chemosensor was investigated (Figure 9). In this study, Ag^+ , Na^+ , K^+ , Ba^{2+} , Ca^{2+} , Co^{2+} , Mg^{2+} , Mn^{2+} , Ni^{2+} , Pb^{2+} , Sn^{2+} , Zn^{2+} , Al^{3+} , Cu^+ , Hg^{2+} and Fe^{3+} (100 μM) were added to the compound L (10 μM)/ Cu^{2+} (50 μM) solution, and the fluorescence was observed. The fluorescence emission intensity at 518 nm significantly decreased as a result of binding with Cu^{2+} . The coexisting ions showed little influence on the detection of Cu^{2+} . Common anions, including oxalate, sulfate, nitrate and chloride, did not interfere with the fluorescence intensity of the ligand or $[\text{L}-\text{Cu}^{2+}]$ complex. Compared to the other common cations, compound L exhibited good selectivity for Cu^{2+} , indicating that L has a good anti-interference ability in detecting Cu^{2+} .

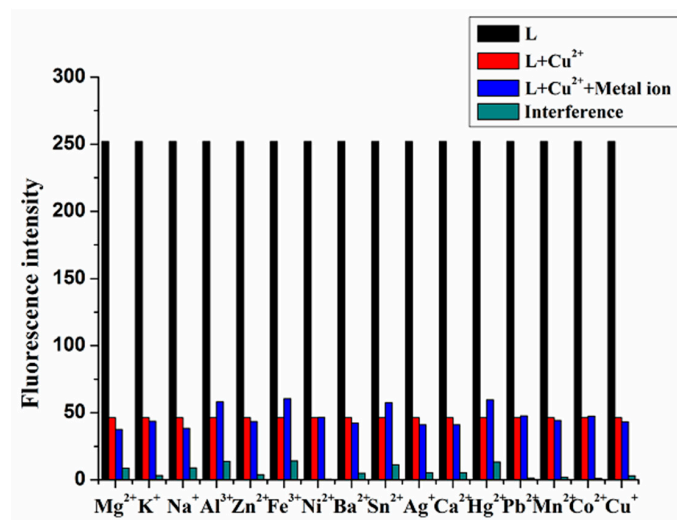


Figure 9. Interference of foreign cations. Solvents: EtOH/ H_2O (4:1 *v/v*).

2.7. Thermal Studies

The stability of probe L and its Cu^{2+} complex was studied by thermogravimetry to prove the binding of ligand L with Cu^{2+} ions, and the results are presented in Figures 10 and 11, respectively. The thermal stability of the Cu^{2+} complex (up to 324.76 $^{\circ}\text{C}$) was better than that of the free ligand (up to 288.57 $^{\circ}\text{C}$).

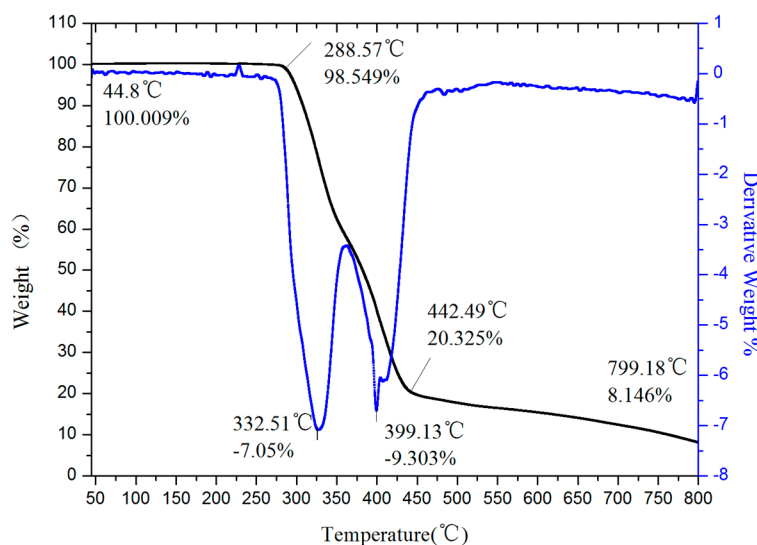


Figure 10. Thermal studies of the fluorescence chemosensor.

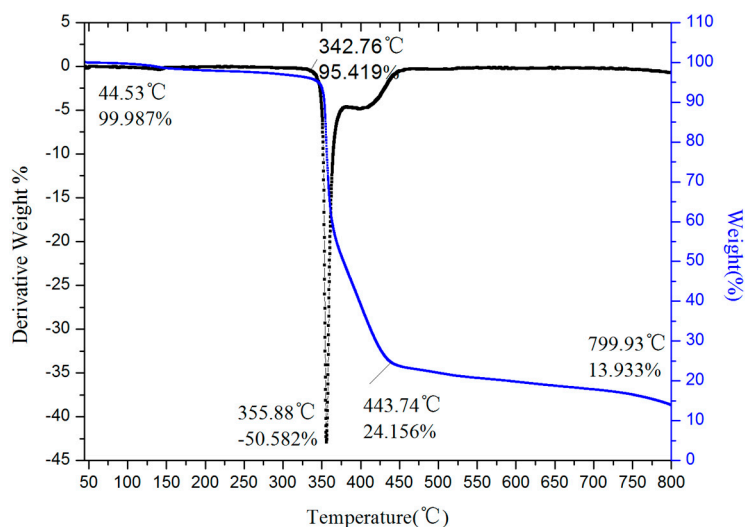


Figure 11. Thermal studies of the $[L-Cu^{2+}]$ complex with the fluorescent chemosensor.

2.8. IR Spectra

The structural matching played an important role in selective recognition. According to the examples in the literature, a similar mode of probes containing a tridentate structure binding with Cu^{2+} has been reported [46,47]. To further study the possible binding mode of compound **L** and Cu^{2+} , IR spectroscopy was employed to elucidate the possible coordination mode. The IR spectra of compound **L** and the $[L-Cu^{2+}]$ complex are compared in Figure 12. The IR spectra of compound **L** (Figure 12a) has two slender peaks appearing between 3350 and 3290 cm^{-1} . One of the extremely sharp peaks in this range vanished when the complex was formed (Figure 12b) and only appeared at 3325.72 cm^{-1} . This result suggested that the aromatic amide was not involved in the coordination of $[L-Cu^{2+}]$. However, the extremely sharp peak in the IR spectra corresponding to the imine disappeared. For fluorescence quenching, the N atom directly connected to naphthalene must be present in the coordination of the complex. On the basis of the aforementioned fact, a plausible binding mode of the complex was proposed, as shown in Scheme 3.

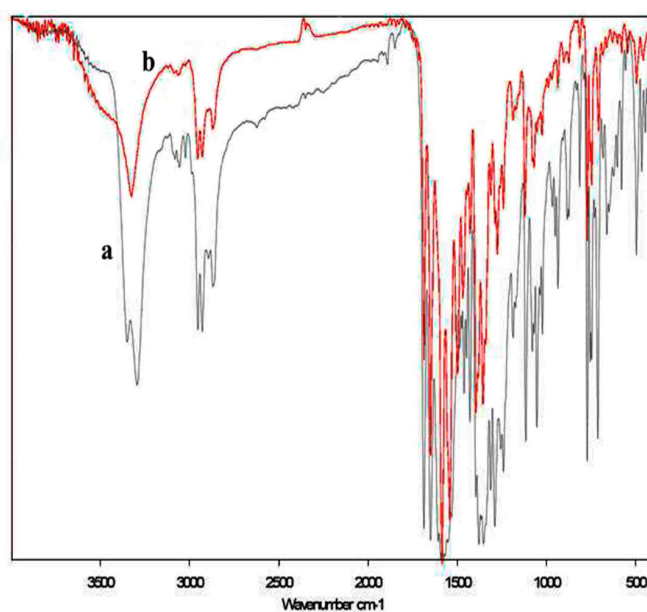
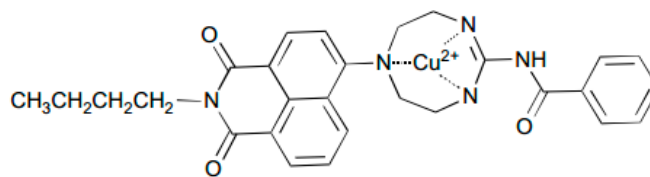


Figure 12. IR spectra of compound **L** before (a) and after (b) the addition of Cu^{2+} .



Scheme 3. Proposed coordination of compound **L** combined with Cu^{2+} .

3. Experimental

3.1. Chemicals and Instruments

All of the solvents and reactants were commercially available and used without purification. The IR spectra were recorded on a Bruker ALPHA-T spectrometer (KBr, BRUKER Inc., Beijing, China). The melting points were determined using a Beijing Taiké melting point apparatus (X-4) and were uncorrected, and $^1\text{H-NMR}$ and $^{13}\text{C-NMR}$ spectra were recorded on a Bruker AVANVE 300 or 400 MHz nuclear magnetic resonance spectrometer (Energy Chemical, Shanghai, China) using CDCl_3 or $\text{DMSO-}d_6$ as the solvent and TMS as the internal standard. The high-resolution mass spectrometry was recorded on a FT-ICR MS spectrometer (BRUKER Inc., Beijing, China). Fluorescence emission spectra were obtained using a PerkinElmer LS55 fluorescence spectrometer (PerkinElmer, Liantrisant, UK). The pH values were measured using a PHS-3C pH meter (Inesa, Shanghai, China). Thermal analysis was performed using a 449F3 thermal analyzer (Netzsch, Bavaria, Germany). The spectrogram data of the synthesized compounds could be found in the Supplementary Materials.

3.2. Testing Methods

Compound **L** was dissolved in EtOH to form a 10^{-3} M stock solution. Cu^{2+} , Ag^+ , Na^+ , K^+ , Ba^{2+} , Ca^{2+} , Co^{2+} , Mg^{2+} , Mn^{2+} , Ni^{2+} , Pb^{2+} , Sn^{2+} , Zn^{2+} , Al^{3+} , Hg^{2+} and Fe^{3+} sources were dissolved in deionized water (H_2O) to obtain 10^{-2} M stock solutions. For the fluorescence measurement of Cu^{2+} , the mixed stock solutions were diluted to 10 mL with EtOH and H_2O to form EtOH/ H_2O (4:1 *v/v*) solutions. For the titration experiments, compound **L** stock solution (100 μL) was mixed with a certain amount of Cu^{2+} stock solution and diluted to 10 mL with EtOH and H_2O to form EtOH/ H_2O (4:1 *v/v*) solutions. The wide pH range solutions were prepared by adjustment of 0.05 mol L^{-1} Tris-HCl solution with HCl or NaOH solution. Thermal studies of compound **L** and its $[\text{L-Cu}^{2+}]$ complex were also performed to prove the binding of the ligand with Cu^{2+} . All fluorescence spectra were recorded at 25°C with the excitation wavelength set at 437 nm and the slit width set at 10 nm.

3.3. Synthesis of *N*-*n*-Butyl-4-bromo-1,8-naphthalimide (**1**)

N-*n*-Butyl-4-bromo-1,8-naphthalimide was prepared according to the reported method [48]. 4-Bromo-1,8-naphthalic anhydride (16.1 g, 58 mmol) and *n*-butyl amine (60 mmol, 4.4 g) were heated under reflux in EtOH (250 mL) with vigorous stirring for 12 h under N_2 . Then, the mixture was cooled, and the precipitate was filtered and recrystallized from ethanol to yield 13.5 g (84%) of a light-yellow product; m.p.: $105\text{--}106^\circ\text{C}$; $^1\text{H-NMR}$ ($\text{DMSO-}d_6$, 300 MHz) δ (ppm): 8.46–8.52 (m, Ar-H, 2H), 8.27 (d, $J = 7.9$ Hz, Ar-H, 1H), 8.16 (d, $J = 7.9$ Hz, Ar-H, 1H), 7.92–7.97 (m, Ar-H, 1H), 4.01 (t, $J = 7.3$ Hz, N- CH_2 , 2H), 1.56–1.66 (m, CH_2 , 2H), 1.31–1.39 (m, CH_2 , 2H), and 0.93 (t, $J = 7.3$ Hz, CH_3 , 3H).

3.4. Synthesis of *N*-*n*-Butyl-4-*N'*,*N'*-dihydroxyethyl-1,8-naphthalimide (**2**)

N-*n*-butyl-4-(*N'*,*N'*-dihydroxyethyl)amino-1,8-naphthalimide was obtained using a procedure similar to that reported by Guo et al. [49]. *N*-*n*-butyl-4-bromine-1,8-naphthalimide (15 g, 45.2 mmol) and diethanolamine (75 mL) were mixed in ethylene glycol monomethyl ether (100 mL). The mixture was refluxed for 6 h. The crude product was purified by column chromatography using silica gel, with EtOAc and light petroleum (1:4 *v/v*) as the eluent. Compound **2** was obtained as a yellow solid

(3.28 g) in a 20% yield; m.p.: 129–130 °C; $^1\text{H-NMR}$ (400 MHz, CDCl_3) δ (ppm): 8.87 (d, $J = 8.8$ Hz, Ar-H, 1H), 8.52 (d, $J = 7.2$ Hz, Ar-H, 2H), 7.66 (t, $J = 8.0$ Hz, Ar-H, 1H), 7.38 (t, $J = 8.0$ Hz, Ar-H, 1H), 4.14 (t, $J = 7.2$ Hz, CH_2 , 2H), 3.87 (t, $J = 5.2$ Hz, CH_2 , 4H), 3.63 (t, $J = 5.2$ Hz, CH_2 , 4H), 2.81 (s, OH, 2H), 1.68–1.69 (m, CH_2 , 2H), 1.43–1.45 (m, CH_2 , 2H), 0.97 (t, $J = 7.2$ Hz, CH_3 , 3H); $^{13}\text{C-NMR}$ (100 MHz, CDCl_3) δ (ppm): 164.34, 163.91, 154.28, 131.18, 131.22, 130.85, 130.14, 127.24, 125.65, 122.92, 117.18, 117.05, 59.73, 59.73, 55.33, 55.33, 40.10, 30.20, 20.38, and 13.85.

3.5. Synthesis of *N-n*-Butyl-4-*N'*,*N'*-diaminoethyl-1,8-naphthalimide (4)

N-n-butyl-4-*N'*,*N'*-diaminoethyl-1,8-naphthalimide was prepared according to the reported procedure [50]. Compound **2** (2.0 g, 5.6 mmol), PPh_3 (4.41 g, 16.8 mmol) and NaN_3 (1.82 g, 28.0 mmol) were dissolved in anhydrous *N,N*-dimethylformamide (100 mL), the solution was cooled to 0 °C, and CBr_4 (5.58 g, 16.8 mmol) was added portionwise over 10 min. Then, the reaction temperature was raised to room temperature, and the mixture was stirred for 12 h. The reaction mixture was diluted with water and extracted with ethyl acetate (4 \times 50 mL). The organic layer was dried over anhydrous Na_2SO_4 and concentrated in vacuo. The crude compound was separated through silica gel column chromatography and afforded compound **3**. The compound **3** (1.9 g, 4.67 mmol) and PPh_3 (7.36 g, 28.1 mmol) were dissolved in 50 mL of pyridine and kept at room temperature for 1 h. Concentrated ammonium hydroxide (10 mL) was added, and the mixture was allowed to stand for an additional 2 h. Pyridine was removed through reduced pressure. Then, CH_2Cl_2 and 1 N HCl were added to the reaction mixture. The organic layer was washed with additional 1 N HCl, and the aqueous layers were combined, neutralized with KOH, and extracted with CH_2Cl_2 . The combined organic layers were washed with water and brine and then dried over anhydrous Na_2SO_4 to afford compound **4** (1.11 g, 67%) as a yellow solid; m.p.: 99–101 °C; $^1\text{H-NMR}$ ($\text{DMSO-}d_6$, 300 MHz) δ (ppm): 8.74 (d, $J = 0.3$ Hz, Ar-H, 1H), 8.43 (d, $J = 7.8$ Hz, Ar-H, 1H), 8.27 (d, $J = 8.4$ Hz, Ar-H, 1H), 7.68 (t, $J = 8.1$ Hz, Ar-H, 1H), 6.81 (d, $J = 8.4$ Hz, Ar-H, 1H), 4.01 (t, $J = 7.8$ Hz, CH_2 , 2H), 3.44–3.48 (m, CH_2 , 2H), 2.87 (t, $J = 5.7$ Hz, CH_2 , 2H), 2.65–2.72 (m, CH_2 , 4H), 1.84 (s, NH_2 , 4H), 1.54–1.62 (m, CH_2 , 2H), 1.30–1.37 (m, CH_2 , 2H), and 0.92 (t, $J = 7.5$ Hz, CH_3 , 3H). HRMS-ESI m/z : found 355.2123 for $[\text{M} + \text{H}]^+$ and calculated 354.2056 for $\text{C}_{20}\text{H}_{26}\text{N}_4\text{O}_2$.

3.6. Synthesis of *N-n*-Butyl-4-(1'-cyclooctene-1',3',6'-triazole)-1,8-naphthalimide (L)

N-n-butyl-4-(1'-cyclooctene-1',3',6'-triazole)-1,8-naphthalimide was obtained using a procedure similar to that reported in the literature [40]. Benzoyl isothiocyanate (0.92 g, 5.6 mmol) was added dropwise to a solution of *N-n*-butyl-4-*N'*,*N'*-diaminoethyl-1,8-naphthalimide (1.0 g, 2.8 mmol) in 30 mL of ketone and was stirred at 45 °C. The reaction mixture was stirred continuously for 45 min. After cooling, the solution was filtered, and the filter cake was washed with EtOH. The crude product was purified by chromatography to afford compound **L** (0.77 g, 57%) as a green solid; m.p.: 165–167 °C; $^1\text{H-NMR}$ (CDCl_3 , 300 MHz) δ (ppm): 9.02 (s, NH, 1H), 8.29–8.42 (m, Ar-H, 4H), 7.54 (d, $J = 6.6$ Hz, Ar-H, 1H), 7.46 (t, $J = 7.5$ Hz, Ar-H, 3H), 6.57 (d, $J = 8.7$ Hz, Ar-H, 2H), 4.12 (t, $J = 7.5$ Hz, CH_2 , 4H), 3.60–3.86 (m, CH_2 , 4H), 3.55–3.61 (m, CH_2 , 2H), 1.63–1.70 (m, CH_2 , 2H), 1.38–1.45 (m, CH_2 , 2H); 1.26 (s, CNHC, 1H), 0.95 (t, $J = 7.5$ Hz, CH_3 , 3H). $^{13}\text{C-NMR}$ (75 MHz, CDCl_3) δ (ppm): 164.72, 164.26, 164.26, 150.97, 150.97, 134.24, 134.24, 131.02, 131.02, 129.54, 129.54, 128.35, 128.35, 128.35, 128.35, 124.25, 122.59, 110.26, 103.13, 103.13, 45.86, 41.31, 41.24, 41.05, 39.93, 30.32, 20.44 and 13.88. HRMS-ESI m/z : found 484.2332 for $[\text{M} + \text{H}]^+$ and calculated 483.5616 for $\text{C}_{28}\text{H}_{29}\text{N}_5\text{O}_3$.

4. Conclusions

In summary, a new, rapidly responsive, colorimetric and “turn-off” fluorescent Cu^{2+} sensor, *N-n*-butyl-4-(1'-cyclooctene-1',3',6'-triazole)-1,8-naphthalimide, was successfully synthesized and characterized. Probe **L** exhibited a markedly quenched fluorescence in the presence of Cu^{2+} with a simultaneous color change (yellow to colorless) over a range of metal cations. The detection was highly sensitive and more selective than some reported probes and almost unaffected by the common

coexisting metal ions [15,51]. In addition, Probe L showed a 1:1 stoichiometry (sensor/Cu²⁺) with a high binding constant. This sensor should be valuable for copper analysis in environmental samples and biological systems.

Supplementary Materials: Supplementary data associated with this article can be found in the online.

Acknowledgments: This work was supported by the Research Science Foundation in Technology Innovation of Harbin (2015RAYXJ010).

Author Contributions: Y. Fu and M.Q. Li developed the concept of the work. Z.Q. Wang and X.M. Liang carried out the synthetic work. Q. Chai conducted the fluorescence properties assay. Q. Chai and F. Ye wrote the paper.

Conflicts of Interest: The authors declare no conflict of interest.

References

1. Thomas, S.W.; Joly, G.D.; Swager, T.M. Chemical sensors based on amplifying fluorescent conjugated polymers. *Chem. Rev.* **2007**, *107*, 1339–1386. [[CrossRef](#)] [[PubMed](#)]
2. Martinez-Manez, R.; Sancenon, F. Fluorogenic and chromogenic chemosensors and reagents for anions. *Chem. Rev.* **2003**, *103*, 4419–4476. [[CrossRef](#)] [[PubMed](#)]
3. Kim, H.N.; Ren, W.X.; Kim, J.S.; Yoon, J. Fluorescent and colorimetric sensors for detection of lead, cadmium, and mercury ions. *Chem. Soc. Rev.* **2012**, *41*, 3210–3244. [[CrossRef](#)] [[PubMed](#)]
4. Duong, T.Q.; Kim, J.S. Fluoro- and chromogenic chemodosimeters for heavy metal ion detection in solution and biospecimens. *Chem. Rev.* **2010**, *110*, 6280–6301. [[CrossRef](#)] [[PubMed](#)]
5. Ding, Y.B.; Tang, Y.Y.; Zhu, W.H.; Xie, Y.S. Fluorescent and colorimetric ion probes based on conjugated oligopyrroles. *Chem. Soc. Rev.* **2015**, *44*, 1101–1112. [[CrossRef](#)] [[PubMed](#)]
6. Lippard, S.J.; Berg, J.M. *Principles of Bioinorganic Chemistry*; University Science Books: Mill Valley, CA, USA, 1994.
7. Que, E.L.; Domaille, D.W.; Chang, C.J. Metals in neurobiology: Probing their chemistry and biology with molecular imaging. *Chem. Rev.* **2008**, *108*, 1517–1549. [[CrossRef](#)] [[PubMed](#)]
8. Thiele, D.J.; Gitlin, A.D. Assembling the pieces. *Chem. Biol.* **2008**, *4*, 145–147. [[CrossRef](#)] [[PubMed](#)]
9. Cho, J.; Pradhan, T.; Lee, Y.M.; Kim, J.S.; Kim, S. A calix[2] Triazole[2] Arene-based fluorescent chemosensor for probing the copper trafficking pathway in Wilson's disease. *Dalton Trans.* **2014**, *43*, 16178–16182. [[CrossRef](#)] [[PubMed](#)]
10. You, G.R.; Park, G.J.; Lee, J.J.; Kim, C. A colorimetric sensor for the sequential detection of Cu²⁺ and CN⁻ in fully aqueous media: Practical performance of Cu²⁺. *Dalton Trans.* **2015**, *44*, 9120–9129. [[CrossRef](#)] [[PubMed](#)]
11. Barnham, K.J.; Masters, C.L.; Bush, A.I. Neurodegenerative diseases and oxidative stress. *Nat. Rev. Drug Discov.* **2004**, *3*, 205–214. [[CrossRef](#)] [[PubMed](#)]
12. Mare, S.; Penugonda, S.; Robinson, S.M.; Dohgu, S.; Banks, W.A.; Ercal, N. Copper complexing decreases the ability of amyloid beta peptide to cross the BBB and enter brain parenchyma. *Peptides* **2007**, *28*, 1424–1432. [[CrossRef](#)] [[PubMed](#)]
13. Kim, B.E.; Nevitt, T.; Thiele, D.J. Mechanisms for copper acquisition, distribution and regulation. *Nat. Chem. Biol.* **2008**, *4*, 176–185. [[CrossRef](#)] [[PubMed](#)]
14. Lee, J.C.; Gray, H.B.; Winkler, J.R. Copper(II) binding to alpha-synuclein, the Parkinson's protein. *J. Am. Chem. Soc.* **2008**, *130*, 6898–6899. [[CrossRef](#)] [[PubMed](#)]
15. Sun, S.H.; Hu, W.T.; Gao, H.F.; Qi, H.L.; Diang, L.P. Luminescence of ferrocene-modified pyrene derivatives for turn-on sensing of Cu²⁺ and anions. *Spectrochim. Acta A* **2017**, *184*, 30–37. [[CrossRef](#)] [[PubMed](#)]
16. Jung, H.S.; Kwon, P.S.; Lee, J.W.; Kim, J.I.; Hong, C.S.; Kim, J.W.; Yan, S.H.; Lee, J.Y.; Lee, J.H.; Joo, T.; et al. Coumarin-derived Cu²⁺-selective fluorescence sensor: Synthesis, mechanisms, and applications in living cells. *J. Am. Chem. Soc.* **2009**, *131*, 2008–2012. [[CrossRef](#)] [[PubMed](#)]
17. Liu, C.X.; Xu, J.; Yang, F.; Zhou, W.; Li, Z.X.; Wei, L.H.; Yu, M.M. Nanomolar Cu²⁺ and F⁻ naked-eye detection with a 1,8-naphthalimide-based colorimetric probe. *Sens. Actuators B* **2015**, *212*, 364–370. [[CrossRef](#)]
18. Khan, B.; Shah, M.R.; Ahmed, D.; Rabnawaz, M.; Anis, I.; Afridi, S.; Makhmoor, T.; Tahir, M.N. Synthesis, characterization and Cu²⁺ triggered selective fluorescence quenching of bis-calix[4]arene tetra-triazole macrocycle. *J. Hazard. Mater.* **2016**, *309*, 97–106. [[CrossRef](#)] [[PubMed](#)]

19. Moussa, H.; Merlin, C.; Dezanet, C.; Balan, L.; Medjandi, G.; Ben-Attia, M.; Schneider, R. Trace amounts of Cu^{2+} ions influence ROS production and cytotoxicity of ZnO quantum dots. *J. Hazard. Mater.* **2016**, *304*, 532–542. [[CrossRef](#)] [[PubMed](#)]
20. Faghihian, H.; Hajishabani, A.; Dadfarnia, S.; Zamani, H. Use of clinoptilolite loaded with 1-(2-pyridylazo)-2-naphthol as a sorbent for preconcentration of Pb(II), Ni(II), Cd(II) and Cu(II) prior to their determination by flame atomic absorption spectroscopy. *Int. J. Environ. Anal. Chem.* **2009**, *89*, 223–231. [[CrossRef](#)]
21. Tomalova, I.; Foltynova, P.; Kanicky, V.; Preisler, J. MALDI MS and ICP MS detection of a single CE separation record: A tool for metalloproteomics. *Anal. Chem.* **2014**, *86*, 647–654. [[CrossRef](#)] [[PubMed](#)]
22. Qing, Z.H.; Mao, Z.G.; Qing, T.P.; He, X.X.; Zou, Z.; He, D.G.; Shi, H.; Huang, J.; Liu, J.B.; Wang, K.M. Visual and portable strategy for copper(II) detection based on a striplike poly(thymine)-caged and microwell-printed hydrogel. *Anal. Chem.* **2014**, *86*, 11263–11268. [[CrossRef](#)] [[PubMed](#)]
23. Liu, Z.M.; Jia, X.L.; Bian, P.P.; Ma, Z.F. A simple and novel system for colorimetric detection of cobalt ions. *Analyst* **2014**, *139*, 585–588. [[CrossRef](#)] [[PubMed](#)]
24. Tang, B.; Niu, J.Y.; Yu, C.G.; Zhuo, L.H.; Ge, J.C. Highly luminescent water-soluble Cd Te nanowires as fluorescent probe to detect copper(II). *Chem. Commun.* **2005**, *33*, 4184–4186. [[CrossRef](#)] [[PubMed](#)]
25. Zhu, Z.Q.; Su, Y.Y.; Li, J.; Li, D.; Zhang, J.; Song, S.P.; Zhao, Y.; Li, G.X.; Fan, C.H. Highly sensitive electrochemical sensor for mercury(II) ions by using a mercury-specific oligonucleotide probe and gold nanoparticle-based amplification. *Anal. Chem.* **2009**, *81*, 7660–7666. [[CrossRef](#)] [[PubMed](#)]
26. Niamnont, N.; Khumsri, A.; Promchat, A.; Tumcharern, G.; Sukwattanasinitt, M. Novel salicylaldehyde derivatives as fluorescence turn-on sensors for cyanide ion. *J. Hazard. Mater.* **2014**, *280*, 458–463. [[CrossRef](#)] [[PubMed](#)]
27. Zhang, J.R.; Zeng, A.L.; Luo, H.Q.; Li, N.B. Fluorescent silver nanoclusters for ultrasensitive determination of chromium(VI) in aqueous solution. *J. Hazard. Mater.* **2016**, *304*, 66–72. [[CrossRef](#)] [[PubMed](#)]
28. Czarnik, A.W. Fluorescent chemosensors for ion and molecule recognition. In *ACS Symposium Series Sponsored by the Division of Organic Chemistry of the American Chemical Society at the 204th Meeting of the American Chemical Society*; American Chemical Society: Washington, DC, USA, 1992; p. 538.
29. Dujols, V.; Ford, F.; Czarnik, A.W. A long-wavelength fluorescent chemodosimeter selective for Cu(II) ion in water. *J. Am. Chem. Soc.* **1997**, *119*, 7386–7387. [[CrossRef](#)]
30. Xiang, Y.; Tong, A.J.; Jin, P.Y.; Ju, Y. New fluorescent rhodamine hydrazone chemosensor for Cu(II) with high selectivity and sensitivity. *Org. Lett.* **2006**, *8*, 2863–2866. [[CrossRef](#)] [[PubMed](#)]
31. Ding, Y.B.; Zhu, W.H.; Xie, Y.S. Development of Ion Chemosensors Based on Porphyrin Analogues. *Chem. Rev.* **2017**, *117*, 2203–2256. [[CrossRef](#)] [[PubMed](#)]
32. Sirilaksanapong, S.; Sukwattanasinitt, M.; Rashatasakhon, P. 1,3,5-Triphenylbenzene fluorophore as a selective Cu^{2+} sensor in aqueous media. *Chem. Commun.* **2012**, *48*, 293–295. [[CrossRef](#)] [[PubMed](#)]
33. Erdemir, S.; Tabakci, B.; Tabakci, M. A highly selective fluorescent sensor based on calix[4]arene appended benzothiazole units for Cu^{2+} , S^{2-} and HSO_4^- ions in aqueous solution. *Sens. Actuators B Chem.* **2016**, *228*, 109–116. [[CrossRef](#)]
34. Hu, Y.; Ke, Q.; Yan, C.; Xu, C.H.; Huang, X.H.; Hu, S.L. A new fluorescence chemosensor for selective detection of copper ion in aqueous solution. *Tetrahedron Lett.* **2016**, *57*, 2239–2243. [[CrossRef](#)]
35. Huang, L.; Cheng, J.; Xie, K.F.; Xi, P.X.; Hou, F.P.; Li, Z.P.; Xie, G.Q.; Shi, Y.J.; Liu, H.Y.; Bai, D.C.; et al. Cu^{2+} -selective fluorescent chemosensor based on coumarin and its application in bioimaging. *Dalton Trans.* **2011**, *40*, 10815–10817. [[CrossRef](#)] [[PubMed](#)]
36. Maher, N.J.; Diao, H.W.; O'Sullivan, J.; Fadda, E.; Heaney, F.; McGinley, J. Lower rim isoxazole-calix[4]arene derivatives as fluorescence sensors for copper(II) ions. *Tetrahedron* **2015**, *71*, 9223–9233. [[CrossRef](#)]
37. Ganguly, A.; Ghosh, S.; Kar, S.; Guchhait, N. Selective fluorescence sensing of Cu(II) and Zn(II) using a simple Schiff base ligand: Naked eye detection and elucidation of photoinduced electron transfer (PET) mechanism. *Spectrochim. Acta Part A* **2015**, *143*, 72–80. [[CrossRef](#)] [[PubMed](#)]
38. Quan, L.; Sun, T.T.; Lin, W.H.; Guan, X.G.; Zheng, M.; Xie, Z.G.; Jing, X.B. Bodipy fluorescent chemosensor for Cu^{2+} detection and its applications in living cells: Fast response and high sensitivity. *J. Fluoresc.* **2014**, *24*, 841–846. [[CrossRef](#)] [[PubMed](#)]
39. Poss, M.A.; Iwanowicz, E.; Reid, J.A.; Lin, J.; Gu, Z.X. A mild and efficient method for the preparation of guanidines. *Tetrahedron Lett.* **1992**, *33*, 5933–5936. [[CrossRef](#)]

40. Liu, B.; Tian, H. A selective fluorescent ratiometric chemodosimeter for mercury ion. *Chem. Commun.* **2005**, 3156–3158. [[CrossRef](#)] [[PubMed](#)]
41. Fischer, M.; Georges, J. Fluorescence quantum yield of rhodamine 6G in ethanol as a function of concentration using thermal lens spectrometry. *Chem. Phys. Lett.* **1996**, *260*, 115–118. [[CrossRef](#)]
42. Ma, Q.J.; Zhang, X.B.; Han, Z.X.; Huang, B.; Jiang, Q.; Shen, G.L.; Yu, R.Q. A ratiometric fluorescent probe for zinc ions based on the quinoline fluorophore. *Int. J. Environ. Anal. Chem.* **2011**, *91*, 74–86. [[CrossRef](#)]
43. Gao, C.J.; Liu, X.; Jin, X.J.; Wu, J.; Xie, Y.J.; Liu, W.S.; Yao, X.J.; Tang, Y. A retrievable and highly selective fluorescent sensor for detecting copper and sulfide. *Sens. Actuators B Chem.* **2013**, *185*, 125–131. [[CrossRef](#)]
44. Karak, D.; Banerjee, A.; Sahana, A.; Guha, S.; Lohar, S.; Adhikari, S.S.; Das, D. 9-Acridone-4-carboxylic acid as an efficient Cr(III) fluorescent sensor: Trace level detection, estimation and speciation studies. *J. Hazard. Mater.* **2011**, *188*, 274–280. [[CrossRef](#)] [[PubMed](#)]
45. Xie, Y.S.; Ding, Y.B.; Li, X.; Wang, C.; Hill, J.P.; Ariga, K.; Zhang, W.B.; Zhu, W.H. Selective, sensitive and reversible “turn-on” fluorescent cyanide probes based on 2,2′-dipyridylaminoanthracene-Cu²⁺ ensembles. *Chem. Commun.* **2012**, *48*, 11513–11515. [[CrossRef](#)] [[PubMed](#)]
46. Wang, H.X.; Yang, L.; Zhang, W.B.; Zhou, Y.; Zhao, B.; Li, X.Y. A colorimetric probe for copper(II) ion based on 4-amino-1,8-naphthalimide. *Inorg. Chim. Acta* **2012**, *381*, 111–116. [[CrossRef](#)]
47. Gao, Y.G.; Tang, Q.; Shi, Y.D.; Zhang, Y.; Lu, Z.L. 1,8-naphthalimide modified [12]aneN compounds as selective and sensitive probes for Cu²⁺ ions and ATP in aqueous solution and living cells. *Talanta* **2016**, *152*, 438–446. [[CrossRef](#)] [[PubMed](#)]
48. Zhang, W.J.; Huo, F.J.; Liu, T.; Wen, Y.; Yin, C.X. A rapid and highly sensitive fluorescent imaging materials for thiophenols. *Dyes Pigm.* **2016**, *133*, 248–254. [[CrossRef](#)]
49. Guo, X.F.; Zhu, B.C.; Liu, Y.Y.; Zhang, Y.; Jia, L.H.; Qian, X.H. Synthesis and properties of N-butyl-4-(aza-15-crown-5)-1, 8-naphthalimide as a fluorescent probe. *Chin. J. Org. Chem.* **2006**, *26*, 504–507.
50. Lee, S.; Lee, J.H.; Pradhan, T.; Lim, C.S.; Cho, B.R.; Bhuniya, S.; Kim, S.; Kim, J.S. Fluorescent turn-on Zn²⁺ sensing in aqueous and cellular media. *Sens. Actuators B Chem* **2011**, *160*, 1489–1493. [[CrossRef](#)]
51. Zheng, X.; Lee, K.H.; Liu, H.G.; Park, S.Y.; Yoon, S.S.; Lee, J.Y.; Kim, Y.G. A bis(pyridine-2-ylmethyl)amine-based selective and sensitive colorimetric and fluorescent chemosensor for Cu²⁺. *Sens. Actuators B Chem.* **2016**, *222*, 28–34. [[CrossRef](#)]

Sample Availability: Samples of the compounds are available from the authors’ lab.



© 2017 by the authors. Licensee MDPI, Basel, Switzerland. This article is an open access article distributed under the terms and conditions of the Creative Commons Attribution (CC BY) license (<http://creativecommons.org/licenses/by/4.0/>).